JOURNAL OF MATERIALS SCIENCE 10 (1975) 613–620

Optical and esr spectra of vanadium (IV) in different simple germanate, phosphate and borate glasses

A. PAUL, F. ASSABGHY*
Department of Glass Technology, University of Sheffield, UK

The optical and esr spectra of some Na_2O–GeO_2, Na_2O–P_2O_5, Na_2O–CaO–P_2O_5 and Na_2O–Al_2O_3–B_2O_3 glasses containing vanadium(IV) have been studied; these spectra have been analyzed by assuming that vanadium(IV) is present as the vanadyl ion in a ligand field of C_{4v} symmetry. It has been found that in Na_2O–GeO_2 and Na_2O–P_2O_5 glasses the covalency in the in-plane V–O δ-bonds increases, and the degree of π-bonding with the vanadyl oxygen decreases, with increasing Na_2O content of the glass; the rate of change being greatest in the region 15 to 20 mol % Na_2O for the Na_2O–GeO_2 series and around 50 mol % in the Na_2O–P_2O_5 series. In the Na_2O–CaO–P_2O_5 glasses the covalency in the in-plane V–O δ-bond decreases and π-bonding with vanadyl oxygen increases on substitution of CaO for Na_2O in the glass. Gradual addition of Al_2O_3 in three different Na_2O–B_2O_3 glasses did not cause any significant change in covalency either in the δ or in the π-bonding. These changes have been discussed in terms of possible structural units in these glasses.

1. Introduction

Optical absorption and esr spectra of vanadium(IV) in different glasses have been studied by various workers [1-5]. Vanadium(IV) has been reported to be in six co-ordinated distorted octahedral symmetry (D_{4h} or even D_{2h} or C_{4v} has been suggested), the degree of distortion being a function of composition of the glass. In this paper we report the esr and optical spectra of vanadium(IV) in different simple glasses of systematically varied compositions. Spin Hamiltonian parameters were calculated from the observed esr spectra assuming that the vanadium(IV) is present as the $(VO)^{2+}$ ion. The covalency in various V–O bonds was then estimated by the method proposed by Hecht and Johnston [2].

2. Experimental

All the raw materials (Na_2CO_3, $NaH_2PO_4.6H_2O$, $CaH_4(PO_4)_2.H_2O$, H_3BO_3, Al_2O_3 and GeO_2) were of Analar grade. Batch materials to produce 10 g glass were accurately weighed, thoroughly mixed in an agate mortar and melted in a Pt + 2% Rh crucible at different temperatures, as shown in Table I. All the glasses were melted for 4 h in an electric furnace with dry air as the furnace atmosphere. The glasses were cast as rectangular slabs and thoroughly annealed. Two sides of the slab were polished and the optical absorption spectrum measured on a Cary 14 spectrophotometer. After absorption measurement the slab was crushed to a coarse powder and used for esr measurement and chemical estimation. All the major components, such as Na_2O, CaO, P_2O_5, B_2O_3, GeO_2 and Al_2O_3 were estimated chemically with conventional methods.

The esr spectra were obtained on a Hilger Watts Microspin spectrometer which operated at about 9200 MHz. The magnetic field was calibrated using a proton resonance probe; the **g** value marker employed was DPPH. The coarsely powdered glass sample was introduced into the resonance cavity in a quartz tube. A typical spectrum is shown in Fig. 1.

The esr spectra obtained were very similar to those reported by other workers, and can be described by means of an axial spin Hamiltonian of the form:

*Permanent address: Department of Materials Engineering and Physical Sciences, The American University in Cairo, Egypt.

TABLE I Composition of glasses and melting temperature

Glass composition (after chemical analysis) (mol%)						Glass no.	Melting temperature (°C)
Na_2O	CaO	Al_2O_3	P_2O_5	B_2O_3	GeO_2		
0	—	—	—	—	100	SGO	—
9.10	—	—	—	—	90.90	SG1	1300
12.49	—	—	—	—	87.51	SG2	1250
18.55	—	—	—	—	81.15	SG3	1200
20.84	—	—	—	—	79.16	SG4	1200
25.82	—	—	—	—	74.18	SG5	1200
28.22	—	—	—	—	71.78	SG6	1100
40.3	—	—	59.7	—	—	SP1	800
50.9	—	—	49.1	—	—	SP2	900
58.7	—	—	41.3	—	—	SP3	900
25.0	25.0	—	50.0	—	—	SCP	1000
—	49.8	—	50.2	—	—	CP	1100
33.33	—	—	—	66.67	—	A1	1000
31.54	—	5.37	—	63.08	—	A2	1000
29.67	—	10.98	—	59.34	—	A3	1050
27.73	—	16.82	—	55.46	—	A4	1100
25.66	—	23.02	—	51.32	—	A5	1150
25.02	—	24.93	—	50.04	—	A6	1150
20.00	—	—	—	80.00	—	B1	1000
18.78	—	6.88	—	74.34	—	B2	1000
18.02	—	9.87	—	72.10	—	B3	1050
17.33	—	13.34	—	69.33	—	B4	1100
14.30	—	—	—	85.70	—	C1	1000
13.89	—	2.90	—	83.21	—	C2	1000
13.33	—	6.81	—	79.86	—	C3	1050
12.75	—	10.84	—	76.41	—	C4	1050

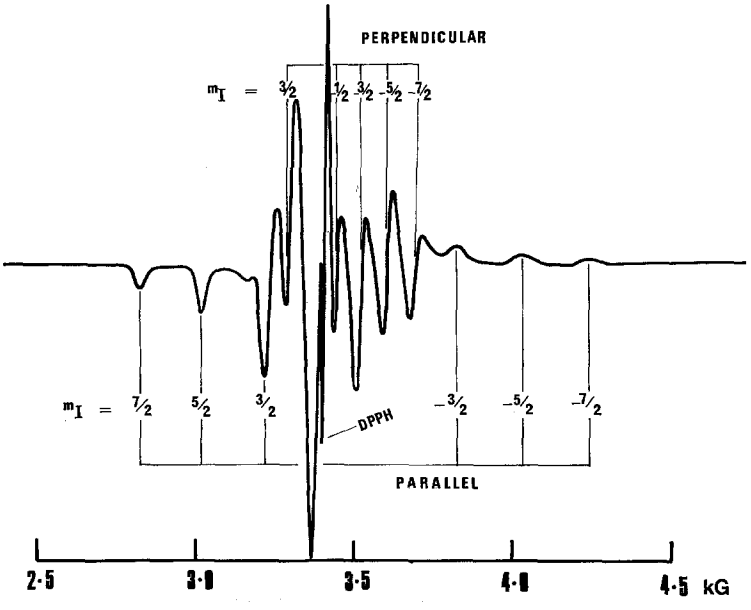

Figure 1 Typical esr spectrum of vanadium(IV) in a Na_2O–GeO_2 glass.

TABLE II Optical and esr parameters of vanadium(IV) in different glasses

Glass no.	$g_{\parallel}$	$g_{\perp}$	$A_{\parallel}$ ($\times 10^3$ cm^{-1})	$A_{\perp}$ ($\times 10^3$ cm^{-1})	$b_2 \rightarrow e_\pi^*$ ($\times 10^3$ cm^{-1})	$b_2 \rightarrow b_1^*$ ($\times 10^3$ cm^{-1})	$(1-\alpha^2)$	$(1-\gamma^2)$
SGO*	1.929	1.976	17.55	6.82	—	13 300	0.03	—
SG1	1.932	1.999	17.04	7.35	10 526	16 800	0.09	0.90
SG2	1.932	1.996	17.42	7.12	10 420	16 670	0.11	0.80
SG3	1.931	1.994	17.20	6.86	10 360	15 380	0.18	0.74
SG4	1.934	1.993	17.18	6.51	10 260	15 150	0.22	0.71
SG5	1.931	1.992	17.10	7.36	10 200	14 200	0.23	0.68
SG6	1.931	1.992	17.10	6.66	10 150	13 750	0.26	0.68
SP1	1.927	1.997	18.59	7.92	11 000	15 130	0.14	0.81
SP2	1.926	1.993	18.03	7.69	11 100	15 150	0.12	0.70
SP3	1.936	1.999	17.64	7.54	11 300	15 000	0.24	0.62
SCP	1.919	1.997	18.33	8.78	11 900	14 490	0.09	0.78
CP	1.919	1.998	18.33	7.93	11 760	14 490	0.08	0.84
A1	1.941 1	1.984 5	17.25	—	10 000	16.950	0.215	0.461
A2	1.941 1	1.985 9	17.47	6.86	10 310	16 950	0.215	0.485
A3	1.942 5	1.988 1	16.97	6.87	10 420	17 090	0.227	0.552
A4	1.942 5	1.988 8	17.36	7.28	11 490	17 090	0.226	0.530
A5	1.942 5	1.992 0	18.96	71.6	14 080	17 240	0.220	0.569
A6	1.942 5	1.993 2	16.89	7.22	—	—	0.220	0.612
B1	1.937 7	1.996 9	17.39	7.22	12 990	16 950	0.171	0.788
B2	1.938 4	1.996 6	17.39	7.25	13 330	17 090	0.170	0.770
B3	1.939 1	1.996 8	17.74	7.03	13 790	17 390	0.168	0.770
B4	1.939 1	1.996 8	17.69	7.27	14 290	17 390	0.171	0.762
C1	1.936 3	1.999 5	17.78	7.48	14 200	17 390	0.160	0.880
C2	1.937 8	1.999 5	18.02	7.57	15 380	17 390	0.151	0.870
C3	1.938 4	1.999 5	17.82	7.41	15 380	17 390	0.159	0.870
C4	1.938 8	1.999 5	14.93	7.64	15 380	17 540	0.157	0.870

*Data taken from [5].

$$\mathscr{H} = \mathbf{g}_{\parallel}\beta S_z H_z + \mathbf{g}_{\perp}\beta(S_x H_x + S_y H_y) + A_{\parallel} S_z I_z + A_{\perp}(S_x I_x + S_y I_y)$$

where β is the Bohr magneton, $g_{\parallel}$ and $g_{\perp}$ are the parallel and perpendicular principal components of the **g**-tensor; $A_{\parallel}$ and $A_{\perp}$ are the parallel and perpendicular components of the hyperfine-coupling tensor; H_x, H_y and H_z are the components of the magnetic field; and S_x, S_y, S_z and I_x, I_y, I_z are the components of the spin operators of the electron and nucleus respectively.

In a glass the resonance condition arising from the above Hamiltonian must be averaged over all values of the angle, θ, which defines the orientation of the magnetic field with respect to the symmetry axis of the axial ion site. The absorption curve in this case is composed of a set of envelopes, one for each $2I + 1$ values of m, whose extreme points occur at the field strengths given by:

$$H_{\parallel} = \frac{2H_0}{g_{\parallel}} - \frac{A_{\parallel}}{g_{\parallel}\beta} \cdot m \quad \text{for } \theta = 0$$

and

$$H_{\perp} = \frac{2H_0}{g_{\perp}} - \frac{A_{\perp}}{g_{\perp}\beta} \cdot m \quad \text{for } \theta = \pi/2$$

where m is the nuclear magnetic quantum number. The extreme points which are relatively pure, can readily be identified on the experimental curve as shown in Fig. 1. The linear plots of $H_{\parallel}$ and $H_{\perp}$ versus the nuclear quantum number, m, has been used to derive the values of the desired parameters: $g_{\parallel}$, $g_{\perp}$, $A_{\parallel}$ and $A_{\perp}$; and these are shown in Table II. Table II also contains the relevant optical transition energies of vanadium(IV) in these glasses as determined from the optical spectrum.

3. Results and discussion

3.1. Na_2O:GeO_2 glasses

The composition of the glasses studied are given in Table I. GeO_2 occurs in two well-defined crystalline forms [6, 7] tetragonal (the rutile structure) and hexagonal (the structure of α-quartz). Glassy GeO_2 is built up of randomly

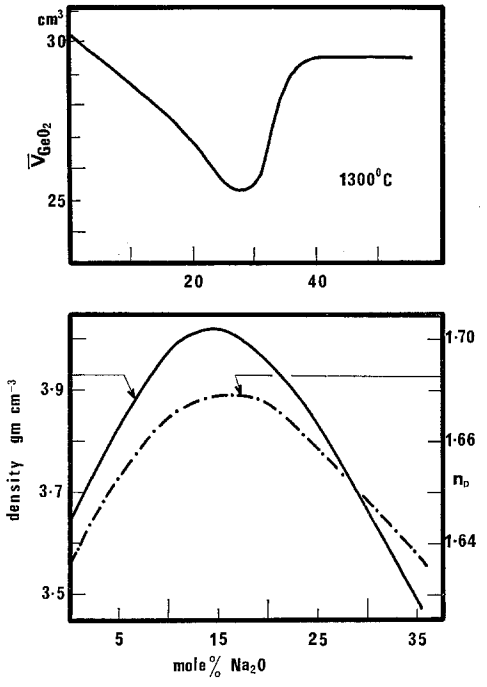

Figure 2 Some physical properties of Na_2O–GeO_2 glasses and melts (density, refractive index and partial molar volume of GeO_2).

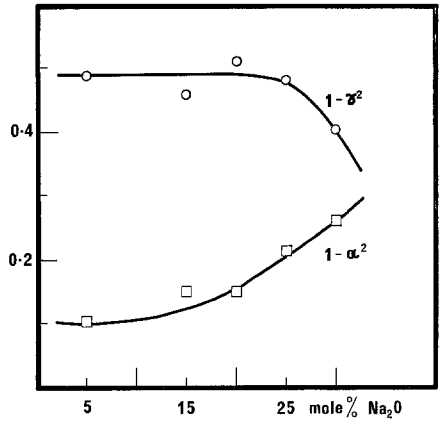

Figure 3 Covalency change of vanadium(IV) in Na_2O–B_2O_3 glasses (after [4]).

oriented GeO_2 tetrahedra with a Ge–O interatomic distance of about 1.65 Å [8]. When Na_2O is added to GeO_2, the co-ordination number of germanium changes from 4 to 6; with further addition of Na_2O, germanium-oxygen tetrahedra with "non-bridging" oxygens are formed [9-12]. Owing to this co-ordination change of germanium and, eventually, formation of non-bridging oxygen in the glass, most of the physical and chemical properties of binary alkali germanates show a non-linear change around 15 to 20 mol % alkali oxide (see Fig. 2). Increase in the co-ordination number of germanium from 4 to 6 involves two high energy d orbitals of germanium for hybridization (sp^3d^2) in place of sp^3 hybridization in GeO_2 tetrahedra. The change in co-ordination and particularly the subsequent formation of non-bridging oxygen in the melt, increases its donor capacity and thus the covalency of vanadium(IV)–oxygen δ-bonding is expected to increase. A similar trend has been observed by Toyuki *et al.* [1] in binary alkali borate glasses whose results on Na_2O–B_2O_3 glasses are shown in Fig. 3.

The bonding scheme of the $(VO)^{2+}$ group according to Ballhausen and Gray [13], is shown in Fig. 4. A very strong δ-bond is formed between the $(2p_z + 2s)$ hybrid of the oxygen and the $(3d_{z^2} + 4s)$ hybrid of the vanadium ion. Since, furthermore, the $2p_x$ and the $2p_y$ orbitals on the oxygen make a strong π-bond with the $3d_{xz}$, $3d_{yz}$ orbitals on the metal ion, vanadium(IV) forms the very stable $(VO)^{2+}$ complex. The $(3d_{z^2} - 4s)$ hybrid, together with the

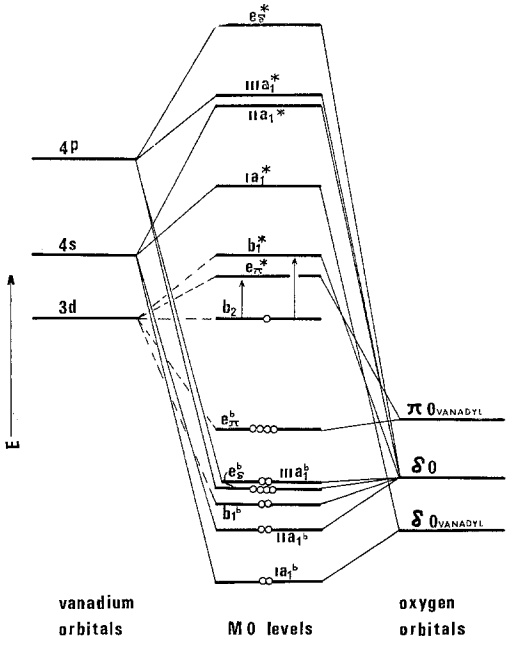

Figure 4 Bonding scheme of $(VO)^{2+}$ group (after [13]).

orbitals $3d_{x^2-y^2}$ and $4p_x$, $4p_y$ and $4p_z$ are then just capable of five δ-bonds directed in a tetragonal pyramid with the vanadium ion located at its base. Thus vanadium(IV) usually occurs in a tetragonally distorted octahedral unit as can be seen from the few examples given in Fig. 5.

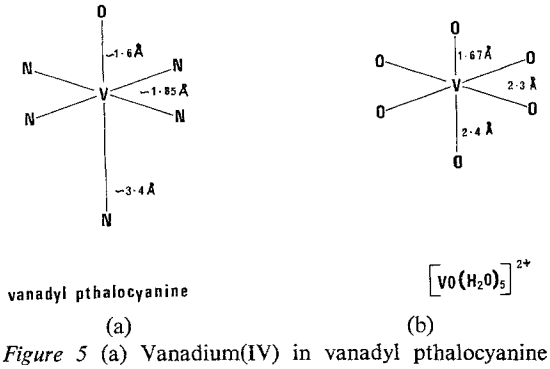

Figure 5 (a) Vanadium(IV) in vanadyl pthalocyanine (after [6]). (b) Vanadium(IV) in $[VO(H_2O)_5]2^+$ complex after [13]).

It is clear from the foregoing discussions that in non-donor solvents like low-alkali germanates or borates, vanadium(IV) will occur predominantly as a $(VO)^{2+}$ group in a tetragonally distorted octahedral unit. As the electron donor capacity of the solvent increases (in the present investigation by adding more Na_2O to GeO_2, P_2O_5 or B_2O_3) the covalency of the in-plane δ-bonds will increase and simultaneously the degree of π-bonding with the vanadyl oxygen will decrease, or in other words the V–O bond length will increase. Thus vanadium(IV) will assume more regular octahedral symmetry with increasing electron donability of the solvent.

The **g** factor measured in this investigation is anisotropic (see Table II) because of the proximity of the e_π^* and b_1^* levels to the b_2 level; the separation energies amongst these levels are given by:

$$g_\perp = g_e\left[1 - \frac{\lambda\gamma^2}{E(b_2 \rightarrow e_\pi^*)}\right]$$

$$g_\parallel = g_e\left[1 - \frac{4\lambda\alpha^2}{E(b_2 \rightarrow b_1^*)}\right]$$

where λ is the spin-orbit coupling constant (165 cm^{-1} [3]), and the expressions $(1 - \alpha^2)$ and $(1 - \gamma^2)$ are degrees of covalency; the covalency increases as $(1 - \alpha^2)$ and $(1 - \gamma^2)$ increases; the former gives an indication of the influence of the δ-bonding between the vanadium ion and the equilateral ligands, while the latter indicates the influence of the π-bondings with the vanadyl oxygen.

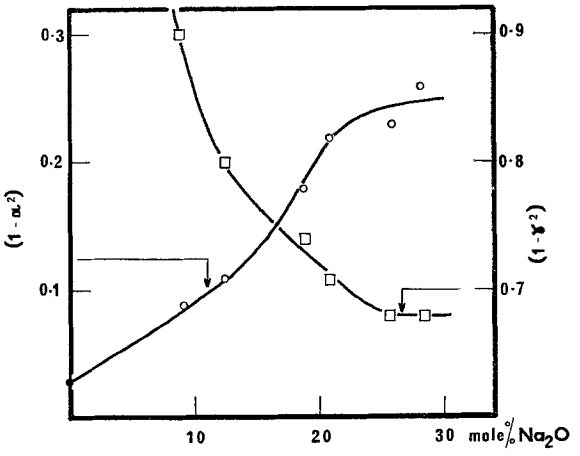

Figure 6 Covalency change of vanadium(IV) in Na_2O–GeO_2 glasses.

The parameters, $(1 - \alpha^2)$ and $(1 - \gamma^2)$ have been calculated for all the glasses and are given in Table II; these are plotted in Fig. 6 against the Na_2O content of the glass. As expected, $(1 - \alpha^2)$ increases and $(1 - \gamma^2)$ decreases with increasing Na_2O, and points of inflection are obtained in both plots around 15 to 20 mol % Na_2O which is consistent with other measured properties of this system of glass.

3.2. Na_2O:P_2O_5 glasses

Attempts to make Na_2O–P_2O_5 glasses containing vanadium(IV) with less than 40 mol % Na_2O were not successful; with small concentrations of total vanadium (less than 0.50 wt %) as was used in the present investigation, glasses containing less than 40 mol % Na_2O, reduced all vanadium to vanadium(III) even when melted at 700°C with oxygen bubbled through the melt. On the other hand, glasses containing more than 60 mol % Na_2O oxidized all vanadium to vanadium (V) under normal conditions of melting; no characteristic optical absorption bands could be observed nor could any esr signal be detected at room temperature.

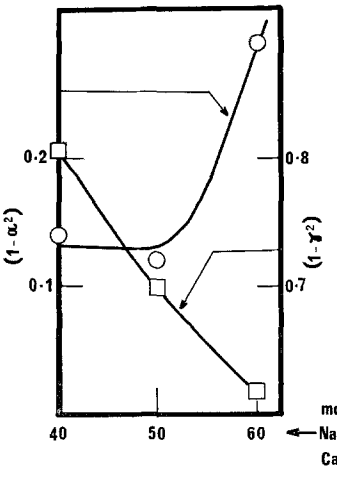

Figure 7

Figure 7 Covalency change of vanadium(IV) in Na_2O–P_2O_5 glasses.

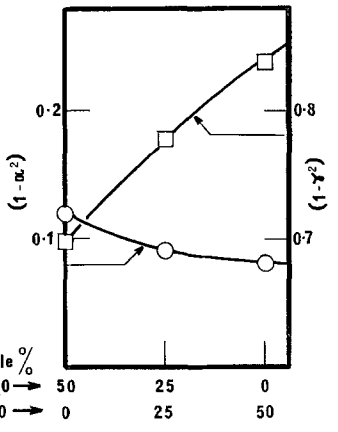

Figure 8

Figure 8 Covalency change of vanadium(IV) in Na_2O–CaO–P_2O_5 glasses.

Vanadium(IV) in Na_2O–P_2O_5 glasses produced very similar esr spectrum as shown in Fig. 1. The optical and esr parameters of vanadium(IV) in these glasses are given in Table II. Variations of $(1 - \alpha^2)$ and $(1 - \gamma^2)$ are plotted in Fig. 7 as a function of composition. As expected the covalency of the in-plane V–O δ-bond increases and that of π-bond with vanadyl oxygen decreases with increasing Na_2O content of the glass. A major change of slope occurs around 50 mol % Na_2O and this is the composition range where predominantly branched phosphate structure converts to infinite chains [14] and consequently the donor capacity of the solvent changes abruptly.

3.3. $Na_2O : CaO : P_2O_5$ glasses

In oxide glass forming melts CaO is less basic than Na_2O; thus substitution of CaO for Na_2O in a Na_2O–P_2O_5 melt decreases donor capacity [15]. The relevant optical and esr parameters of vanadium(IV) in Na_2O–CaO–P_2O_5 glasses are given in Table II. The variation of $(1 - \alpha^2)$ and $(1 - \gamma^2)$ as a function of composition is plotted in Fig. 8. As expected, the degree of covalency in the in-plane V–O bond decreases and simultaneously that of π-bonding with vanadyl oxygen increases on substitution of CaO for Na_2O in the metaphosphate glasses.

3.4. $Na_2O : Al_2O_3 : B_2O_3$ glasses

Na_2O in B_2O_3 produces tetrahedral boron [16]; and with larger amounts of Na_2O (more than 20 mol %) "non-bridging" oxygen on three coordinated boron along with tetrahedral boron are formed [17]. The reactions involved can be schematically represented as:

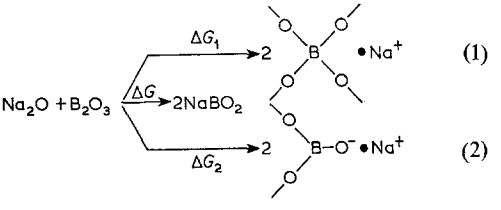

(1)

(2)

The exact magnitudes of ΔG_1 and ΔG_2 are not known, but from NMR results [16] where concentration of tetrahedral boron in glass can be estimated with reasonable accuracy, it appears that up to 35 mol % Na_2O, $\Delta G_1 > \Delta G_2$. Al_2O_3 also can combine with Na_2O as follows:

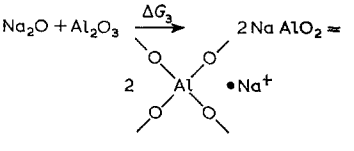

(3)

The standard values of Gibbs free energy, ΔG and ΔG_3 are shown in Fig. 9. Unfortunately, these do not provide the possibility of evaluating the reaction constants under the present conditions

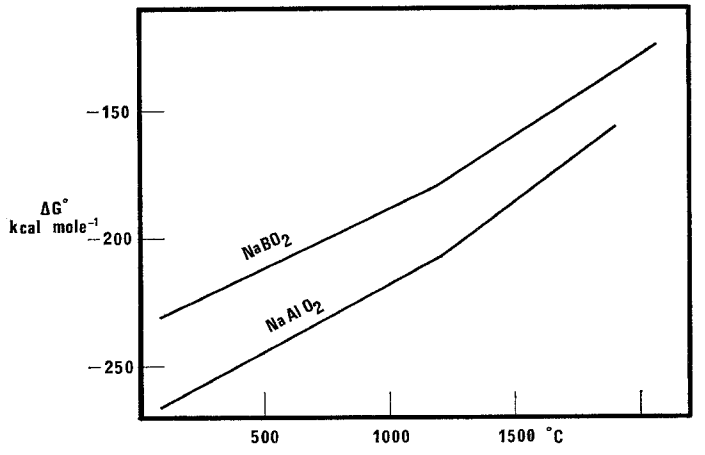

Figure 9 Standard free energy of formation of $NaBO_2$ and $NaAlO_2$.

of melting and subsequent annealing. However, the extremely large (150 to 250 kcal mol^{-1}) changes in free energy leave no doubt of the near completeness of Reactions 1-3 given above. Combining reactions 1 and 3:

$$2\,NaBO_2 + Al_2O_3 \overset{K}{\rightleftharpoons} 2\,NaAlO_2 + B_2O_3 \quad (4)$$

$$K = \frac{a^2_{(NaAlO_2)} \cdot a_{(B_2O_3)}}{a^2_{(NaBO_2)} \cdot a_{(Al_2O_3)}} . \quad (5)$$

No sensible deductions can be made from the free energy change of Reaction 4 only unless at least some qualitative information is available as to how the activity coefficients of the different species written in Equation 5 vary with composition of the melt. In an analogous system, $CaO–Al_2O_3–B_2O_3$ Bray *et al.* [18] have determined the concentration of four-coordinated boron as a function of Al_2O_3 content. Some of their results are shown in Table III; it is clear that both Al_2O_3 and B_2O_3 compete for CaO of the melt, and the free energy changes of the individual reactions are comparable. This is in contrast with $Na_2O–Al_2O_3–SiO_2$ glasses where Na_2O has been reported to be exclusively involved with Al_2O_3 in preference to SiO_2 [19, 20].

TABLE III Concentration of tetrahedral boron and tetrahedral aluminium in 25CaO, xAl_2O_3, (75-x) B_2O_3 glasses (after [18])

Composition (mol %)			Fraction of four co-ordinated	
CaO	Al_2O_3	B_2O_3	Boron	Aluminium
25	0	75	0.351 ± 0.030	—
25	10	65	0.247 ± 0.016	0.895
25	15	60	0.173 ± 0.019	0.975
25	20	55	0.154 ± 0.009	0.826
25	25	50	0.103 ± 0.010	0.794

Three series of $Na_2O–Al_2O_3–B_2O_3$ glasses containing vanadium(IV) have been studied. The composition of glasses are shown in Fig. 10; relevant optical and esr parameters of vanadium(IV) in these glasses are given in Table II. From the $(1 - \alpha^2)$ and $(1 - \gamma^2)$ plots in Figs. 11 and 12 it is clear that addition of Al_2O_3 did not cause any significant changes either in the

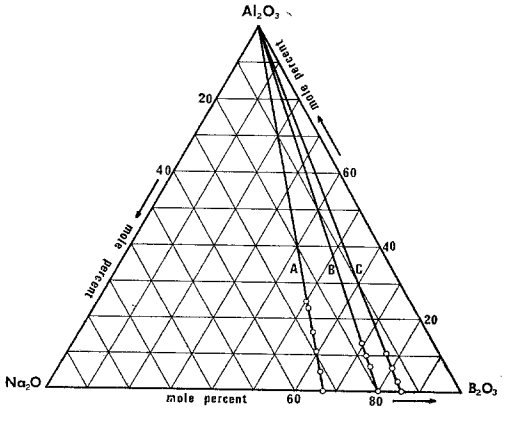

Figure 10 Composition of $Na_2O–Al_2O_3–B_2O_3$ glasses (mol %).

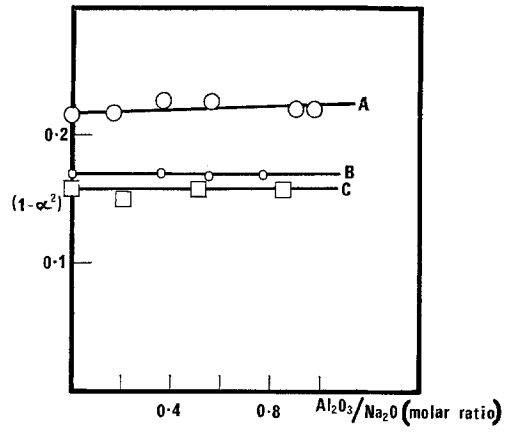

Figure 11 Covalency change of vanadium(IV) in Na_2O–Al_2O_3–B_2O_3 glasses.

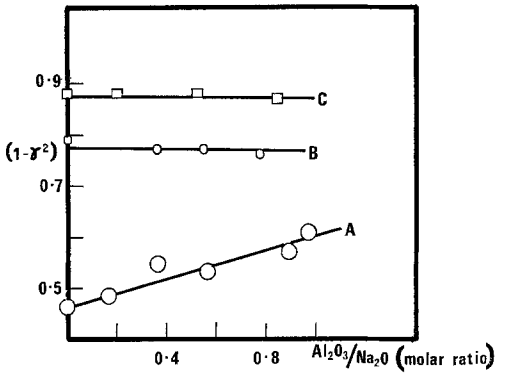

Figure 12 Covalency change of vanadium(IV) in Na_2O–Al_2O_3–B_2O_3 glasses.

in-plane δ-bonding or in the π-bonding with the vanadyl oxygen, although decrease of Na_2O in binary Na_2O–B_2O_3 glasses causes a large change in both $(1 - \alpha^2)$ and $(1 - \gamma^2)$ (for example compare glasses A1, B1 and C1). In glass A6 the ratio Al_2O_3/Na_2O is almost unity but $(1 - \alpha^2)$ is very similar to that of glass A1 which contains the same Na_2O/B_2O_3 ratio but no Al_2O_3. From the foregoing discussions there is very little doubt that addition of Al_2O_3 in a Na_2O–B_2O_3 melt has produced considerable amounts of tetrahedral aluminium at the expense of boron tetrahedra. Assuming Reaction 4 to be nearly complete, in glass A6 concentration of tetrahedral aluminium is about half that of total boron polyhedra (triangular + tetrahedral). It is hard to conceive that even with this large concentration of aluminium tetrahedra, vanadium(IV) is exclusively co-ordinated with boron polyhedra and this co-ordination sphere is independent of aluminium concentration in the melt. The possible operating mechanism seems to be that in Na_2O–Al_2O_3–B_2O_3 glasses vanadium(IV) is co-ordinated with both boron and aluminium polyhedra, the number of ligated aluminium tetrahedra increases with increasing aluminium concentration in the melt. Aluminium tetrahedra and boron tetrahedra possess the same donor capacity towards bonding with vanadium(IV) in these glasses. Thus no net changes in covalency is observed in these glasses with variable Al_2O_3 but constantNa_2O/B_2O_3 ratio.

References

1. H. TOYUKI and S. AKAGI, *Phys. Chem. Glasses* **13** (1972) 15.
2. H. G. HECHT and T. S. JOHNSTON, *J. Chem. Phys.* **46** (1967) 23.
3. D. KIVELSON and S. LEE, *ibid* **41** (1964) 1896.
4. G. HOCHSTRASSER, *Phys. Chem. Glasses* **7** (1966) 178.
5. I. SIEGEL, *Phys. Rev.* **134** (1964) A193.
6. W. ZACHARIASEN, *Z. Krist.* **67** (1928) 226.
7. R. SCHWARTZ and E. HASCHKE, *Z. Anorg. Allgem. Chem.* **252** (1943) 170.
8. J. ZARZYCKI, *Verres Refract.* **11** (1957) 3.
9. E. F. RIEBLING, *J. Chem. Phys.* **39** (1963) 1889, 3022.
10. A. O. IVANOV and K. S. EPSTROPIEV, *Dokl. Akad. Nauk. SSSR* **145** (1962) 797.
11. M. K. MURTHY and J. IP, *Nature* **4916** (1964) 285.
12. M. K. MURTHY and E. M. KIRBY, *Phys. Chem. Glasses* **5** (1964) 144.
13. C. J. BALLHAUSEN and H. B. GRAY, *Inorg. Chem.* **1** (1962) 111.
14. A. E. R. WESTMAN, "Modern Aspects of vitreous state", Vol. 1, edited by J. D. Mackenzie (Butterworths, London, 1960) p. 63.
15. A. PAUL, *J. Non-cryst. Solids*, in press.
16. P. J. BRAY and J. G. O'KEEFE, *Phys. Chem. Glasses* **4** (1963) 37.
17. A. PAUL and R. W. DOUGLAS, *ibid* **8** (1967) 151.
18. S. G. BISHOP and P. J. BRAY, *ibid* **7** (1966) 73.
19. J. O. ISARD, *J. Soc. Glass Technol.* **43** (1959) 113T.
20. D. E. DEY and G. E. RINDONE, *J. Amer. Ceram. Soc.* **45** (1962) 489.

Received 23 September and accepted 18 November 1974.